OAK RIDGE
NATIONAL
LABORATORY

MARTIN MARIETTA

ORNL/TM-10192

The Oak Ridge Heat Pump Design Model: Mark III Version Program Documentation

S. K. Fischer
C. K. Rice
W. L. Jackson

OPERATED BY
MARTIN MARIETTA ENERGY SYSTEMS, INC.
FOR THE UNITED STATES
DEPARTMENT OF ENERGY

Printed in the United States of America. Available from
National Technical Information Service
U.S. Department of Commerce
5285 Port Royal Road, Springfield, Virginia 22161
NTIS price codes—Printed Copy: A03 Microfiche A01

ORNL/TM-10192

Energy Division

THE OAK RIDGE HEAT PUMP DESIGN MODEL: MARK III VERSION PROGRAM DOCUMENTATION

S. K. Fischer
C. K. Rice
W. L. Jackson

Date Published - March 1988

OAK RIDGE NATIONAL LABORATORY
Oak Ridge, Tennessee 37831
operated by
MARTIN MARIETTA ENERGY SYSTEMS, INC.
for the
U.S. DEPARTMENT OF ENERGY
under contract DE-AC05-84OR21400

CONTENTS

EXECUTIVE SUMMARY

Oak Ridge National Laboratory (ORNL) is a leader in the development of analytical tools for the design of electrically driven, air-to-air heat pumps. Foremost among these tools is the ORNL Heat Pump Design Model, which can be used to predict the steady-state heating and cooling performance of an electrically driven, air-source heat pump. Copies of this program have been sent to industry, university, and government research laboratories where the program has been used extensively in energy conservation research. The ORNL Heat Pump Design Model has continued to evolve since the users' manual for the program, ORNL/CON-80/R1, was last revised in August 1983. This series of modifications to the heat pump model has resulted in the Mark III Version, which is three to five times faster, easier to use, and more versatile than earlier versions and can be executed on a personal computer.

The major changes made to earlier versions of the heat pump model relate to the organization of the input data, elimination of redundant calculations in the compressor and refrigerant property computations, improvement of thermostatic expansion valve (TXV) and capillary tube correlations, revision of output format, and modifications to enable the model to run on a personal computer. The input data were rearranged so that data logically related to other data are now read in together. The compressor calculations were modified to eliminate an unnecessary iteration, and two of the refrigerant property subroutines were changed to reduce computer time requirements. The correlations used to model TXVs and capillary tubes were changed to be of more general use. The output summary format was modified to be more useful and readable. Finally, the code was compiled and linked to run on an IBM PC or compatible personal computer. This last change included adding subroutines that give a visual representation of the input and output data on the computer monitor as well as a detailed printed listing of the heat pump simulation. The documentation includes newly developed program structure and solution logic diagrams to aid user understanding of the program.

The Mark III Version of the ORNL Heat Pump Design Model is a comprehensive program for the simulation of an electrically driven, air-source heat pump. The recent program changes make it both faster and easier to use, and the capability to run on a personal computer is a new feature.

ABSTRACT

Oak Ridge National Laboratory (ORNL) is a leader in the development of analytical tools for the design of electrically driven, air-to-air heat pumps. Foremost among these tools is the ORNL Heat Pump Design Model, which can be used to predict the steady-state heating and cooling performance of an electrically driven, air-source heat pump. The ORNL Heat Pump Design Model has continued to evolve since the users' manual for the program, ORNL/CON-80/R1, was last revised in August 1983. This series of modifications to the heat pump model resulted in the Mark III Version, which is three to five times faster, easier to use, and more versatile than earlier versions and can be executed on a personal computer.

The major changes made to earlier versions of the heat pump model relate to the organization of the input data, elimination of redundant calculations in the compressor and refrigerant property computations, improvement of thermostatic expansion valve and capillary tube correlations, revision of output format, and modifications to enable the model to run on a personal computer. The Mark III Version of the ORNL Heat Pump Design Model is a comprehensive, easy-to-use program for the simulation of an electrically driven, air-source heat pump.

INTRODUCTION

The Oak Ridge National Laboratory (ORNL) Heat Pump Design Model is a FORTRAN IV computer program to simulate the steady-state performance of an electrically driven, air-to-air, heat pump. It has been the subject of reports by Ellison and Creswick,[1] Rice et al.,[2] Rice and Fischer,[3] and Fischer and Rice.[4,5] The program has undergone important revisions since the users' manual was first published in 1981 and revised in 1983 (ref. 4). These modifications had been documented for internal use,[5,6] but because of extensive and ongoing distribution of the program, this report was needed to serve as documentation more suitable for external distribution.

CHANGES IN THE HEAT PUMP MODEL

Main Program

The DRIVER routine was improved by adding comments, removing outdated error messages, and improving the error message that is used when any of the three main program loops fail to converge. The evaporator air temperature convergence loop in the main program was improved so that it uses the most recent slope if the initial step size does not bracket a solution.

Compressor Routines

The major structural change to the program was to reformulate the sequence of the compressor calculations. Previously, the user was required to make starting guesses for the saturation temperatures at the condenser inlet and evaporator exit and for the refrigerant mass flow rate. The user also specified the low-side superheat at the evaporator exit. The compressor subroutine then had to evaluate the conditions at the compressor inlet and exit, beginning with these initial estimates, by iteratively calculating the pressure and temperature changes in the connecting lines.

The revised version of the compressor model is based on conditions at the shell inlet and outlet, and the computations proceed outward to the heat exchangers. This reformulation eliminated the costly iteration on conditions in the refrigerant lines and produced a faster-running code that gives the same results. Starting guesses are now specified for the saturation temperatures at the compressor shell inlet and exit, and the superheat is now given at the compressor shell inlet. An estimate of the refrigerant mass flow rate is no longer needed. The required evaporator exit superheat is computed in the compressor model and passed to the evaporator and thermostatic expansion valve (TXV) routines where it is used as described in ORNL/CON-80/R1 (ref. 4). The changes in the input data (e.g., the starting guesses) are reflected in the variable definitions contained in Appendix A.

Flow Control Models

The TXV model in the heat pump model was modified to correct some errors in the earlier releases and to make it more general. Equation 5.6 in ORNL/CON-80/R1 (ref. 4) was found to be not general enough. The user is now required to specify the maximum effective superheat value (which had been computed by Eq. 5.6). The TXV distributor information was modified so that the distributor tube length is now set in BLOCK DATA, rather than in the TXV routine. The TXV routine was further modified to allow separate values to be built in for the sizes of the distributor nozzle for heating and cooling modes.

The previous release of the program did not account for the TXV bleed factor effects properly. For calculating flow through a given TXV, now Eq. 5.5 in ref. 4 is -

$$\dot{m}_{r,TXV} = \left[C_{TXV}(\Delta T_{oper} - \Delta T_{static}) + C_{bleed}\right](\rho_r \Delta P)^{1/2} , \qquad (5.5R)$$

where

$$C_{bleed} = \left[(b_{fac} - 1)\dot{m}_{r,rated}\right] / (\rho_r \Delta P)^{1/2}_{rated} .$$

The bleed factor term, b_{fac}, is now dropped from Eq. 5.7 in ref. 4 for $\dot{m}_{r,rated}$.

For calculating the rated size given the actual refrigerant flow, the rated mass flow rate computed by Eq. 5.21 in ref. 4 was accordingly replaced by Eq. 5.20R, i.e.,

$$\dot{m}_{r,rated} = \frac{\dot{m}_{r,TXV}(\rho_r \Delta P)^{1/2}_{rated}}{\left[\dfrac{\Delta T_{oper} - \Delta T_{static}}{\Delta T_{rated} - \Delta T_{static}} + (b_{fac} - 1)\right](\rho_r \Delta P)^{1/2}_{TXV}} . \qquad (5.20R)$$

The TXV flow coefficient from Eq. 5.20 in ref. 4 is now computed using Eq. 5.21R.

$$C_{TXV} = \dot{m}_{r,rated} \Big/ \left[(\Delta T_{rated} - \Delta T_{static})(\rho_r \Delta P)^{1/2}_{rated}\right] . \qquad (5.21R)$$

The new TXV equations account for the true displacement (slope and intercept) of the flow vs operating superheat curve with various bleed factors, as shown in Fig. 1, rather than just giving a slope change around the static superheat intercept as was the case previously.

ORNL-DWG 86-8013

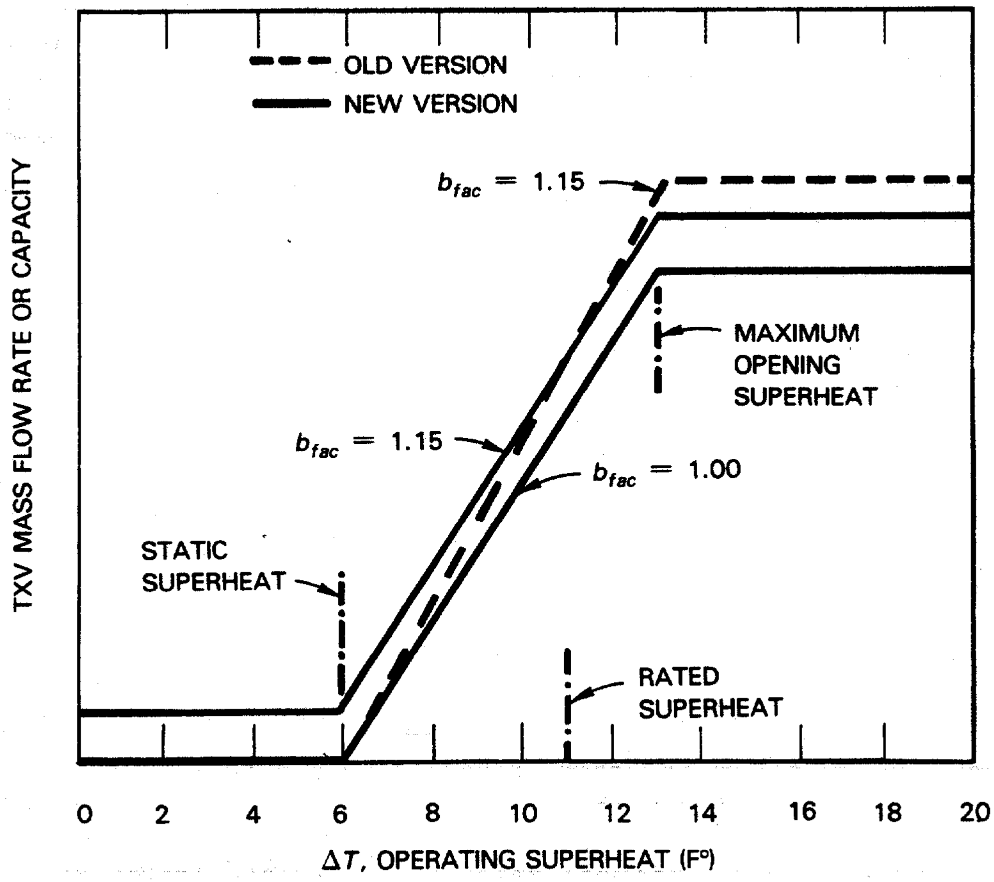

Fig. 1. TXV performance characteristics vs valve operating superheat.

The iterations on mass flow rate for the TXV now use a step size of 6, instead of 1.5, in the call from DRIVER. This was found to improve the TXV version running time. The TXV loop to update the refrigerant pressure entering the evaporator was found to be working incorrectly. This was fixed by setting the variable ITRPIE to 1 after statement number 560 in DRIVER.

Another change that was made as part of the efforts to validate the heat pump model was to extend the capillary tube correlations to handle two-phase refrigerant at the capillary tube inlet. The equations for this are based on an empirical fit to the capillary tube flow factor curves in the ASHRAE Handbook.[7]

The only input definition change, besides the TXV maximum opening input involves suction line heat transfer. We have found that the TXV iterations can become unstable sometimes with suction line heat transfer specified as a rate. In the revised version, the user can specify a fixed suction line temperature rise by giving the negative of the desired value in place of the suction heat gain input on card 19. This alternative input prevents the evaporator superheat from changing within the TXV mass flow iteration loop.

Contact Conductance

In the past, the contact conductance was computed just at the point of contact for uncollared fins in the heat exchangers. The heat transfer resistance equations in the heat exchanger models have been changed so that the contact conductance resistance is applied along the entire length of the tube, as would be appropriate for collared fins. Also, in the past, the user was required to specify values for the contact conductance, but now an algorithm is built into the program. This uses a correlation by Eckels[8] in which the contact conductance is a function of the fin thickness, fin spacing, and the outside diameter of the tube. The contact conductance for a wet coil is increased by a factor of 1.33 as suggested by Eckels.

Because we found that the heat transfer correlations already implicitly contain contact conductance effects, we are now recommending that the contact conductance equations added to the heat pump model be overridden by using a large multiplier, such as 100, for the appropriate input values on cards 13 and 17 of the new input data. We hope to eventually obtain some heat transfer correlations with these effects separated, but until then use of the given contact conductance equations essentially amounts to counting these effects twice.

Refrigerant Property Calculations

This revised version of the heat pump model was used at ORNL to perform numerical optimizations of heat pump design for maximum seasonal performance. These studies required thousands of calls on the steady-state program; a quick check of the calculations showed that a great deal of the computer time was being spent in the refrigerant properties routines. Figures B.1 through B.8 in Appendix B show the "hierarchical structure" of the subroutine calls where the subroutines in the leftmost columns of Figs. B.3 through B.8 call the routines connected to them to the right, and these in turn call those connected to the right of them.

Though TSAT and SPVOL are very concise, efficient subroutines, they are called very often (see the figures in Appendix B for the hierarchies of subroutine calls). We found that a third to a half of the execution time for a heat pump simulation was spent in these two subroutines. In fact they are called frequently with identical values for the parameters as in the previous call. A straightforward change was made to these two subroutines to save some of the effort that was being put into repetitive calls to them. The arguments, or parameters, that are used in calling the subroutines are compared with those used the last time that subroutine was called. If they are the same, the answer that was previously calculated is returned. If they are different, the correct answers are calculated and saved for the next comparison, and these new answers are returned to the calling program. Although this is a "brute-force" way of eliminating repetitive calculations and does not save the overhead required in calling the subroutines, even so it reduces overall running time of the heat pump model by 30 to 40%.

These changes to TSAT and SPVOL were made by storing the old parameter values and old solutions in common blocks. Thereby, as "global" symbols, they would not be lost through any overlays or changes in numerical registers. Initial values for these "past iteration" values are assigned in TABLES.

Subroutine TRIAL was also modified to replace a bisection convergence scheme with a more efficient root-finding program, ZEROON. This saved an additional 5 to 10% in computational time.

Air-Side Heat Transfer Coefficients

Next, the subroutine HAIR was modified slightly to better handle cases where the limits of the heat transfer correlation are exceeded. Previously, if the Reynolds number was outside of the range 3000 to 15,000, a warning was printed and either the lower limit of the range (if the Reynolds number was below 3000) or the upper limit was used to compute the air-side heat transfer coefficient. The new version of HAIR uses the computed Reynolds number; it does not set the Reynolds number to one of the two limits. This change to HAIR eliminates a discontinuity that had been introduced into the correlations. However, the change may also give unreasonable values for the air-side heat transfer coefficient, and therefore it is recommended that any results obtained using the correlations outside the proper range on the Reynolds number be used with caution. The warning message is still given to alert the user to this possibility.

Evaporator Iterations

The iterative calculations in the evaporator subroutine, EVAPR, occasionally had difficulty converging on the specified level of superheat. The logic structure of these computations was modified to alleviate, if not eliminate altogether, this difficulty.

Changes to Common Blocks

Changes were also made to a number of common blocks. PRNT8 was eliminated altogether, and the variables that had been stored in it have been split between two new common blocks, MAINVL and FANMOD. BLANK COMMON, which had contained TITLE; DDUCT, and FIXCAP, was replaced by a common block named TITLE, containing the array TITLE; DDUCT was moved to common block AIR; and FIXCAP was moved to MAINVL.

Input Data

The input data for the heat pump model were left relatively unchanged, but they were reorganized to get a more logical grouping of variables. The new order of input data is described in Appendix A.

The input routine DATAIN was also modified to include data that will be used when a charge inventory model is included in the heat pump model. This version of the code does not include the charge calculations; it merely provides a structure for the input that will be required later. These changes in the input data are described in Appendix A so that a different data file format for the charge inventory version currently under development at ORNL would not be required later.

Work in validating the heat pump model with laboratory data convinced us that it would be useful to be able to specify measured fan powers directly, as an alternative, rather than always calculating them. Otherwise, all the computations are interwoven and it is tedious to correct heat exchanger capacities for fan power differences when one is studying agreement with experimental data. Also the limitations of the fan and air-side pressure drop models sometimes make overriding with direct fan power values preferable. The revised version of the model permits the fan powers to be specified through the fan efficiency variables as described in Appendix A.

Output Routines

WRITE statements and FORMATS were changed throughout the program so that the printed output would be more useful (especially for diagnostic cases where LPRINT>2).

Subroutines SUMCAL and SUMPRT have been added to the heat pump model. They replace summary calculations and output functions that previously were done in the main program.

SUMCAL is called from the main program DRIVER at the end of each loop of the iteration on the evaporator inlet air temperature. It is used to compute the steady-state heat pump capacity, the coefficient of performance (COP), and the energy efficiency ratio (EER) (in cooling mode), as well as the system performance values, including backup resistance heat required to meet an optional user-specified house load. Energy input values are also converted to watts to be transferred to SUMPRT. Two new common blocks, MAINVL and WATTS, were set up to contain all the primary performance values that are transferred to SUMPRT. These common blocks will also be used to transfer steady-state performance data to other driving programs [such as the ORNL

Annual Performance Factor (APF)/Loads Model] that might invoke the steady-state program.

SUMPRT is used to print a one-page summary of the steady-state performance. It is called from DRIVER if the print control variable LPRINT is not equal to 1 and from OUTPUT if LPRINT is equal to 1. This is shown in Fig. B.3. The information printed by SUMPRT includes:

* a summary of the inlet-air and compressor-saturated refrigerant temperatures,
* an energy input summary,
* a refrigerant-side summary,
* an energy output summary, and
* heat pump and system (i.e., with backup heat) performance values.

This information is presented in a more concise, readable form than was the case in earlier releases of the model.

PROGRAM DISTRIBUTION

The ORNL heat pump model is available, free of charge, for use on mainframe and microcomputers. It is distributed on either a 9-track, 1600-bpi magnetic tape or on four dual-sided double-density floppy disks. The microcomputer or personal computer version of the program is identical to the mainframe version, with a few minor exceptions. (All common blocks were removed to a single file and INCLUDE statements are used in their place in each subroutine.) The personal computer version was developed using IBM Professional FORTRAN, which requires that the computer have a math coprocessor (either the 8087 or 80287).

The program will run on a floppy-disk-based IBM PC or PC compatible computer, but a hard disk is necessary for modifying and relinking the FORTRAN code. The object module library that is used is a very large file and fills more than half of a floppy disk. The MS-DOS utility for maintaining object file libraries, LIB, automatically makes a backup file each time the library is updated. It is not possible to do this with the heat pump model using a floppy disk because there is not enough space on the disk for the backup file.

Subroutines have been added to the personal computer version of the code to sketch a rough "schematic" of the refrigerant loop on the monitor screen and to label symbols for the compressor and heat exchangers with input and output data. This is in addition to the standard printed output.

FUTURE PROGRAM MODIFICATIONS

Current program logic is shown in Fig. 2. Work is progressing on adding charge inventory calculations to the Mark III version of the program. That logic will follow the logic shown in Fig. 3. Some planned improvements to the fan models, new reversing valve models, better

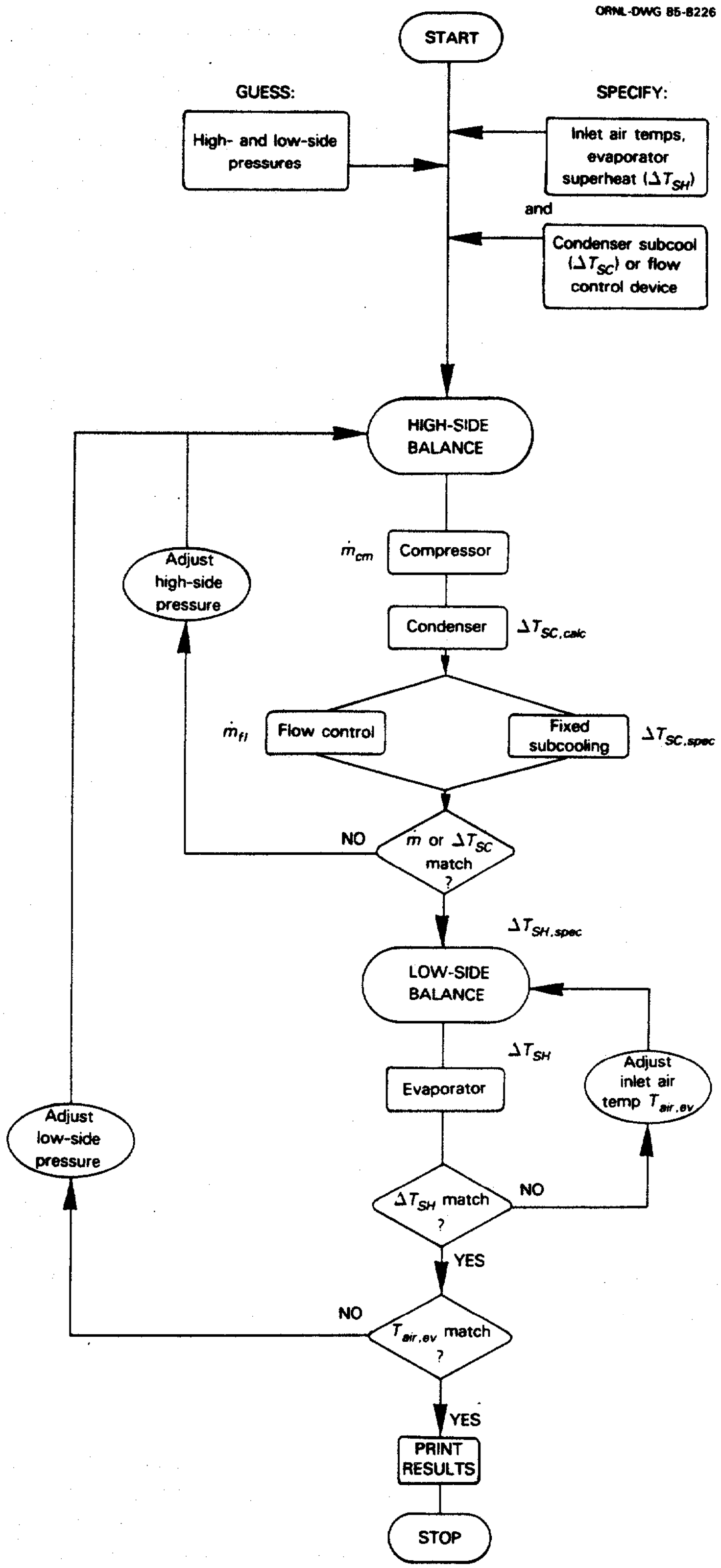

Fig. 2. Solution logic of ORNL heat pump model.

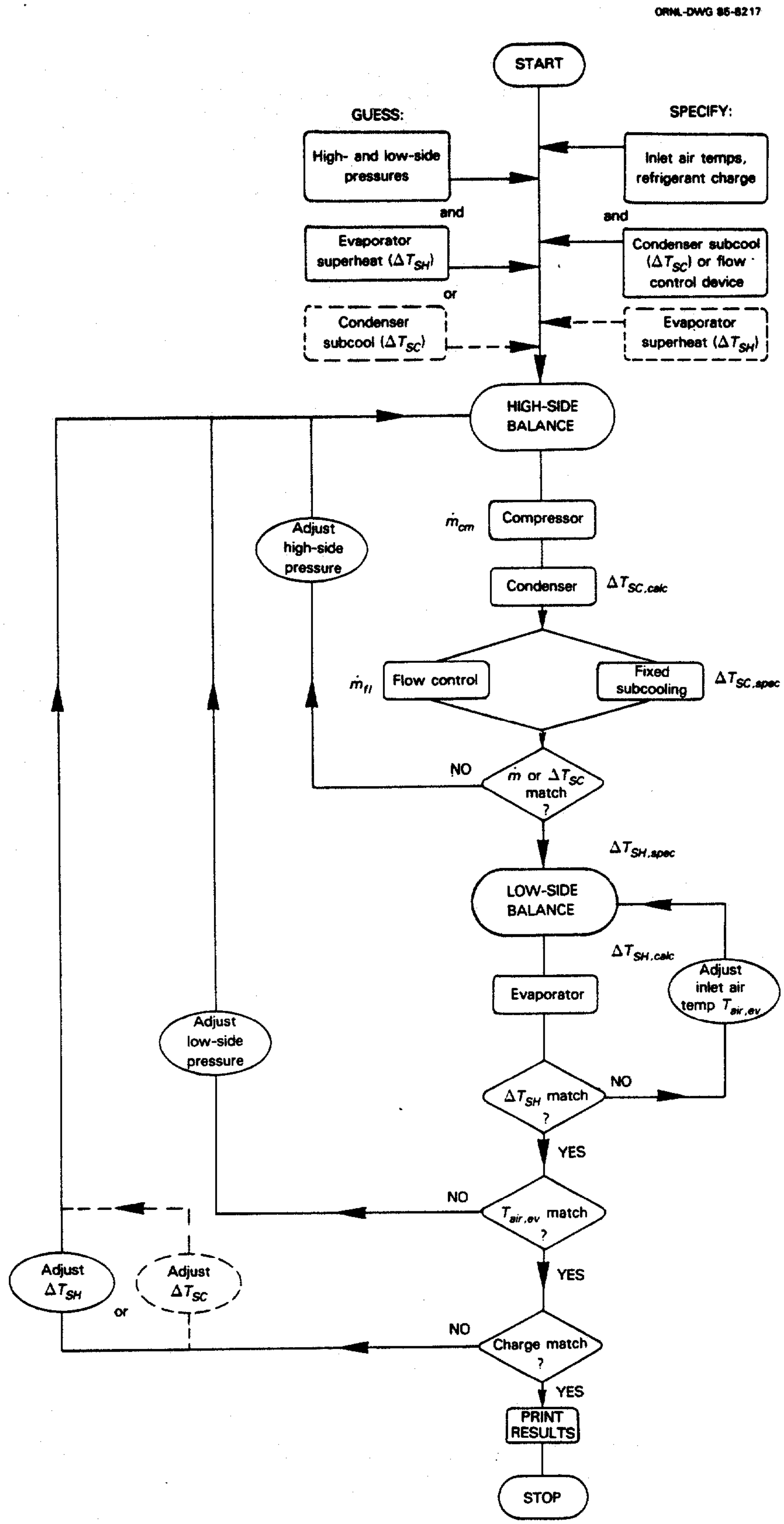

Fig. 3. ORNL heat pump model with charge inventory.

wavy-fin heat exchanger correlations, and the charge inventory calculations will complete a second, general distribution version of the heat pump model that will supersede the program described in ORNL/CON-80/R1 (ref. 4).

REFERENCES

1. R. D. Ellison and F. A. Creswick, A Computer Simulation of Air-to-Air Heat Pumps, ORNL/CON-16, Oak Ridge National Laboratory, March 1978.

2. C. K. Rice et al., Design Optimization and the Limits of Steady-State Heating Efficiency for Conventional Single-Speed Air-Source Heat Pumps, ORNL/CON-63, Oak Ridge National Laboratory, October 1981.

3. C. K. Rice and S. K. Fischer, "A Comparative Analysis of Single- and Continuously Variable Capacity Heat Pump Concepts," pp. 57-65, Proceedings of the DOE/ORNL Heat Pump Conference: Research and Development on Heat Pumps for Space Conditioning Applications, Washington, D.C., Dec. 11-13, 1984, CONF-841231, Oak Ridge National Laboratory, August 1985.

4. S. K. Fischer and C. K. Rice, The Oak Ridge Heat Pump Models: I. A Steady-State Computer Design Model for Air-to-Air Heat Pumps, ORNL/CON-80/R1, Oak Ridge National Laboratory, August 1983.

5. C. K. Rice, private communication to P. D. Fairchild and S. K. Fischer, September 1984.

6. C. K. Rice, private communication to V. D. Baxter and S. K. Fischer, July 1985.

7. ASHRAE Equipment Handbook, 1975, Chapter 20, pp. 20.20 through 20.27.

8. P. W. Eckels, "Contact Conductance of Mechanically Expanded Plate Finned Tube Heat Exchangers," presented at AIChE-ASME Heat Transfer Conference, Salt Lake City, Utah, August 1977.

Appendix A

INPUT DATA DESCRIPTIONS

TITLE, OUTPUT, and MODE DATA

<u>CARD #1</u> <u>FORMAT(20A4)</u>

ITITLE Descriptive title for system described by this set of data

<u>CARD #2</u> <u>FORMAT(8I10)</u>

LPRINT Output switch to control the detail of printed results 1

=0, for minimum output with only an energy input and output summary printed
=1, for a summary of the system operating conditions and component performance calculations as well as the energy summary
=2, for output after each intermediate iteration converges
=3, for continous output during intermediate iterations

<u>CARD #3</u> <u>FORMAT(8I10)</u>

NCORH Switch to specify cooling or heating mode 2

=1, for cooling mode
=2, for heating mode

SUPERHEAT / CHARGE INVENTORY DATA:

<u>CARD #4</u> <u>FORMAT(I10,7F10.4)</u>

ICHRGE Switch for specifying compressor inlet superheat or system refrigerant charge 0

=0, specify refrigerant superheat (or quality) and compute the required system refrigerant charge

=1, estimate compressor inlet superheat and specify the system refrigerant charge, <u>not yet available</u>

SUPER if ICHRGE=0, the specified refrigerant superheat (or quality) at the compressor shell inlet (F^{o} or negative of the desired quality fraction), 18.7
if ICHRGE=1, an estimate of the refrigerant superheat (or quality) at the compressor shell inlet (F^{o} or negative of the desired quality fraction)

Variable Used Only If ICHRGE=1

REFCHG	Specified system refrigerant charge (lbm)	

FLOW CONTROL DEVICE DATA: the variables on the next card depend on the type of flow control device selected.

CARD #5 FORMAT(I10,7F10.4)

Fixed Condenser Subcooling:

IREFC	=0, for specified refrigerant subcooling at the condenser exit	0
DTROC	the specified refrigerant subcooling (or quality) at the condenser exit (F^o or negative of the desired quality fraction)	44.2

Thermostatic Expansion Valve:

IREFC	=1, for the thermostatic expansion valve	1
TXVRAT	The rated capacity of the TXV (tons)	2.0
STATIC	The static superheat setting for the TXV (F^o)	6.0
SUPRAT	The TXV superheat at rating conditions (F^o)	11.0
SUPMAX	The maximum effective operating superheat (F^o)	13.0
BLEEDF	The TXV bypass or bleed factor	1.15
NZTBOP	A switch to omit TXV nozzle and tube pressure drop calculations =0.0, to omit tube and nozzle pressure drops =1.0, to include tube and nozzle pressure drop calculations	0.0

Capillary Tube:

IREFC	=2, for a capillary tube expansion device	2
CAPFLO	The capillary tube flow factor, see ASHRAE Guide and Data Book, Equipment Vol. (1975), Fig. 41, p. 20.25	2.2
NCAP	The number of capillary tubes in parallel	1.0

Short Tube Orifice:

IREFC	=3, for a short tube orifice	3
ORIFD	The diameter of the short-tube orifice (in.)	0.0544

ESTIMATES OF THE LOW AND HIGH SIDE REFRIGERANT SATURATION TEMPERATURES:

CARD #6 FORMAT(8F10.4)

TSICMP	Estimate of the refrigerant saturation temperature at the compressor inlet (^{o}F)	30.0
TSOCMP	Estimate of the refrigerant saturation temperature at the compressor outlet (^{o}F)	115.0

COMPRESSOR DATA:

CARD #7 FORMAT(I10,7F10.4)

ICOMP	Switch to specify which compressor submodel is to be used, =1, for the efficiency and loss model, =2, for the map-based model	2
DISPL	Total compressor piston displacement (in.^{3})	4.520
SYNC	The synchronous compressor motor speed (rpm) when ICOMP=1 and FLMOT is specified on CARD #9;	(3600.)
	the rated compressor motor speed (rpm) when ICOMP=1 and FLMOT is to be calculated or when ICOMP=2	3450.
QCAN	The compressor shell heat loss rate (Btu/h), used if CANFAC=0.0	0.0
CANFAC	Switch to control the method of specifying the compressor shell heat loss rate, QCAN =0.0, to specify QCAN explicitly <1.0, to calculate QCAN as a fraction of the compressor input power, POW, (i.e., QCAN = CANFAC · POW) 1.0, to calculate QCAN from the equation: QCAN = 0.90 · (1 - motor · mechanical efficiency) · POW	0.35

EFFICIENCY AND LOSS MODEL COMPRESSOR DATA:

<u>CARD #8</u> <u>FORMAT(8F10.4)</u>

VR	Compressor actual clearance volume ratio	0.06
EFFMMX	Maximum efficiency of the compressor motor	0.82
ETAISN	Isentropic efficiency of the compressor	0.70
ETAMEC	Mechanical efficiency of the compressor	0.80

<u>CARD #9</u> <u>FORMAT(I10,7F10.4)</u>

MTRCLC	Switch to determine whether to calculate the full load motor power (FLMOT) or to use the input value =0, to calculate FLMOT =1, to use the input value of FLMOT	0
FLMOT	Compressor motor output at full load (kW) (not used if MTRCLC=1)	(2.15)
QHILO	Heat transfer rate from the compressor inlet line to the inlet gas (Btu/h), used if HILOFC=0.0	300.0
HILOFC	Switch to determine internal heat transfer from the high side to the low side, QHILO =0.0, to specify QHILO explicitly <1.0, to calculate QHILO = HILOFC · POW 1.0, to calculate QHILO = 0.03 · POW	0.0

MAP-BASED COMPRESSOR MODEL INPUT DATA:

<u>CARD #8</u> <u>FORMAT(8E10.3)</u>

CPOW(1)	Coefficient for the second-order term in condensing temperature for the compressor power consumption	-1.509E-04
CPOW(2)	Coefficient for the linear term in condensing temperature for the compressor power consumption	4.089E-02

CPOW(3)	Coefficient for the second-order term in evaporating temperature for the compressor power consumption	-1.338E-04
CPOW(4)	Coefficient for the linear term in evaporating temperature for the compressor power consumption	5.860E-04
CPOW(5)	Coefficient for the cross-term in condensing and evaporating temperatures for the compressor power consumption	3.638E-04
CPOW(6)	Constant term in the fit to compressor power consumption as a function of condensing and evaporating temperatures (kW)	9.759E-05
DISPLB	Base compressor displacement for the compressor map (in.^{3})	4.520E+00
SUPERB	Base 'superheat' value for the compressor map if positive, the base superheat entering the compressor (F^o);	20.00E+00
	if negative, the negative of the return gas temperature into the compressor (F^o)	(-95.00E+00)

CARD #9 FORMAT(8E10.3)

CXMR(1)	Coefficient for the second-order term in condensing temperature for the refrigerant mass rate	-2.675E-02
CXMR(2)	Coefficient for the linear term in condensing temperature for the refrigerant mass flow rate	4.633E-00
CXMR(3)	Coefficient for the second-order term in evaporating temperature for the refrigerant mass flow rate	4.703E-02
CXMR(4)	Coefficient for the linear term in evaporating temperature for the refrigerant mass flow rate	9.640E-00
CXMR(5)	Coefficient for the cross-term in condensing and evaporating temperatures for the refrigerant mass flow rate	-1.868E-02
CXMR(6)	Constant term in the fit to refrigerant mass flow rate as a function of condensing and evaporating temperatures (lbm/h)	1.207E-04

INDOOR COIL DATA:

CARD #10 FORMAT(8F10.4)

TAIII	Air temperature entering the heat exchanger (°F)	70.0
RHI	Relative humidity of the air entering the heat exchanger	0.50

CARD #11 FORMAT(8F10.4)

QAI	Air flow rate (ft^3/min)	1230.0
FANEFI	<1.0, the specified value of the combined fan and fan motor efficiency	(0.153)
	>1.0, the specified value of the fan power (watts)	608.0
DDUCT	Diameter of each of six identical air ducts with equivalent lengths of 100 ft (in.)	8.00
FIXCAP	House heating load (Btu/h), optional, used to calculate the necessary backup resistance heat in heating mode	15000.

CARD #12 FORMAT(8F10.4)

AAFI	Frontal area of the coil (ft^2)	3.1667
NTI	Number of refrigerant tube rows in the direction of the air flow	3.0
NSECTI	Number of equivalent, parallel refrigerant circuits in the heat exchanger	3.0
WTI	Spacing of the refrigerant tubes in the direction of the air flow (in.)	0.875
STI	Spacing of the refrigerant tube passes perpendicular to the direction of the air flow (in.)	1.00
RTBI	Total number of return bends in the heat exchanger (all circuits)	72.0

CARD #13 FORMAT(8F10.4)

FINTYI	Switch to specify the type of fin surface, =1.0, for smooth fins =2.0, for wavy fins =3.0, for louvered fins	2.0
FPFI	Fin pitch (fins/in.)	14.0
DELTAI	Fin thickness (in.)	0.00550
DEAI	Outside diameter of the refrigerant tubes (in.)	0.392
DERI	Inside diameter of the refrigerant tubes (in.)	0.360
XKFI	Thermal conductivity of the fin material (Btu/h-ft-^{o}F)	128.3
XKTI	Thermal conductivity of the tube material (Btu/h-ft-^{o}F)	225.0
HCONTI	Fraction or multiple of the default computed contact conductance between the fins and tubes	100.0

OUTDOOR COIL DATA:

CARD #14 FORMAT(8F10.4)

TAIIO	Air temperature entering the heat exchanger (^{o}F)	41.7
RHO	Relative humidity of the air entering the heat exchanger	0.50

CARD #15 FORMAT(8F10.4)

QAO	Air flow rate (ft^3/min)	2300.0
FANEFO	<1.0, the specified value of the combined fan and fan motor efficiency	(0.114)
	>1.0, the specified value of the fan power (watts)	511.0
MFANFT	Switch for using static efficiency vs specific speed curve fit for the efficiency of the outdoor fan, =0, use the specified value of FANEFO as described above =1, use the curve fit for fan static efficiency and the fixed fan motor efficiency value given in BLOCK DATA	0

CARD #16 FORMAT(8F10.4)

AAFO	Frontal area of the coil (ft^2)	5.040
NTO	Number of refrigerant tube rows in the direction of the air flow	3.0
NSECTO	Number of equivalent, parallel refrigerant circuits in the heat exchanger	4.0
WTO	Spacing of the refrigerant tubes in the direction of the air flow (in.)	0.875
STO	Spacing of the refrigerant tube passes perpendicular to the direction of the air flow (in.)	1.00
RTBO	Total number of return bends in the heat exchanger (all circuits)	64.0

CARD #17 FORMAT(8F10.4)

FINTYO	Switch to specify the type of fin surface, =1.0, for smooth fins =2.0, for wavy fins =3.0, for louvered fins	2.0
FPO	Fin pitch (fins/in.)	14.0
DELTAO	Fin thickness (in.)	0.00550
DEAO	Outside diameter of the refrigerant tubes (in.)	0.392
DERO	Inside diameter of the refrigerant tubes (in.)	0.360
XKFO	Thermal conductivity of the fin material (Btu/h-ft-°F)	128.3
XKTO	Thermal conductivity of the tube material (Btu/h-ft-°F)	225.0
HCONTO	Fraction or multiple of the default computed contact conductance between the fins and tubes	100.0

CONFIGURATION OPTIONS DATA:

CARD #18 FORMAT(8I10)

MCMPOP	Switch for adding compressor can heat loss to air across the outdoor coil, =0, compressor can loss not added to outdoor air =1, compressor can loss added to air before crossing the outdoor coil =2, compressor can loss added to air after crossing the outdoor coil	0
MFANIN	Switch for adding heat loss from the indoor fan to air stream, settings are similar to those for MCMPOP	1
MFANOU	Switch for adding heat loss from the outdoor fan to air stream, settings are similar to those for MCMPOP	2

REFRIGERANT LINES DATA:

CARD #19 FORMAT(8F10.4)

Heat Transfer in Refrigerant Lines

QSUCLN	If positive, the rate of heat gain in the compressor suction line (Btu/h),	242.
	If negative, the negative of the desired temperature rise in the suction line (^{o}F)	-3.0
QDISLN	Rate of heat loss in the compressor discharge line (Btu/h)	1648.
QLIQLN	Rate of heat loss in the liquid line (Btu/h)	433.

CARD #20 FORMAT(8F10.4)

Lines Between Coils and from Reversing Valve to Coils

DLL	Inside diameter of the liquid line (in.)	0.194
XLEQLL	Equivalent length of the liquid line (ft)	30.4
DLRVIC	Inside diameter of the vapor line between the reversing valve and the indoor coil (in.)	0.550

XLRVIC	Equivalent length of the vapor line between the reversing valve and the indoor coil (ft)	30.1
DLRVOC	Inside diameter of the vapor line between the reversing valve and the outdoor coil (in.)	0.686
XLRVOC	Equivalent length of the vapor line between the reversing valve and the outdoor coil (ft)	6.0

CARD #21 FORMAT(8F10.4)

Lines from the Reversing Valve to the Compressor

DSLRV	Inside diameter of the suction line from the reversing valve to the compressor inlet (in.)	0.686
XLEQLP	Equivalent length of the low-pressure line from the reversing valve to the compressor inlet (ft)	2.0
DDLRV	Inside diameter of the discharge line from the compressor outlet to the reversing valve (in.)	0.555
XLEQHP	Equivalent length of the high-pressure line from the compressor outlet to the reversing valve (ft)	2.0

Appendix B

HIERARCHY OF SUBROUTINE CALLS

Figures B.1 through B.8 show the hierarchy of subroutine calls in the Mark III version of the ORNL Heat Pump Design Model. Figure B.1 summarizes the overall computational structure of the program; Fig. B.2 summarizes the structure of the refrigerant thermodynamic property and psychrometric routines referenced by shorthand notation in Fig. B.1. Subroutines underlined in Fig. B.1 denote instances of parallel structure between condenser and evaporator and between different compressor and flow control models.

Figures B.3 through B.8 break down the information in Figs. B.1 and B.2 into smaller, easier-to-follow pieces. Figure B.3 illustrates the subroutines called directly from the main program, DRIVER, and references the other figures for the compressor models (Fig. B.4), condenser and evaporator models (Figs. B.5 and B.7), and the flow control calculations (Fig. B.6). Further detail of the evaporator computations are shown in Fig. B.8 (this parallels condenser calculations that are included in Fig. B.5).

ORNL-DWG 86-8017

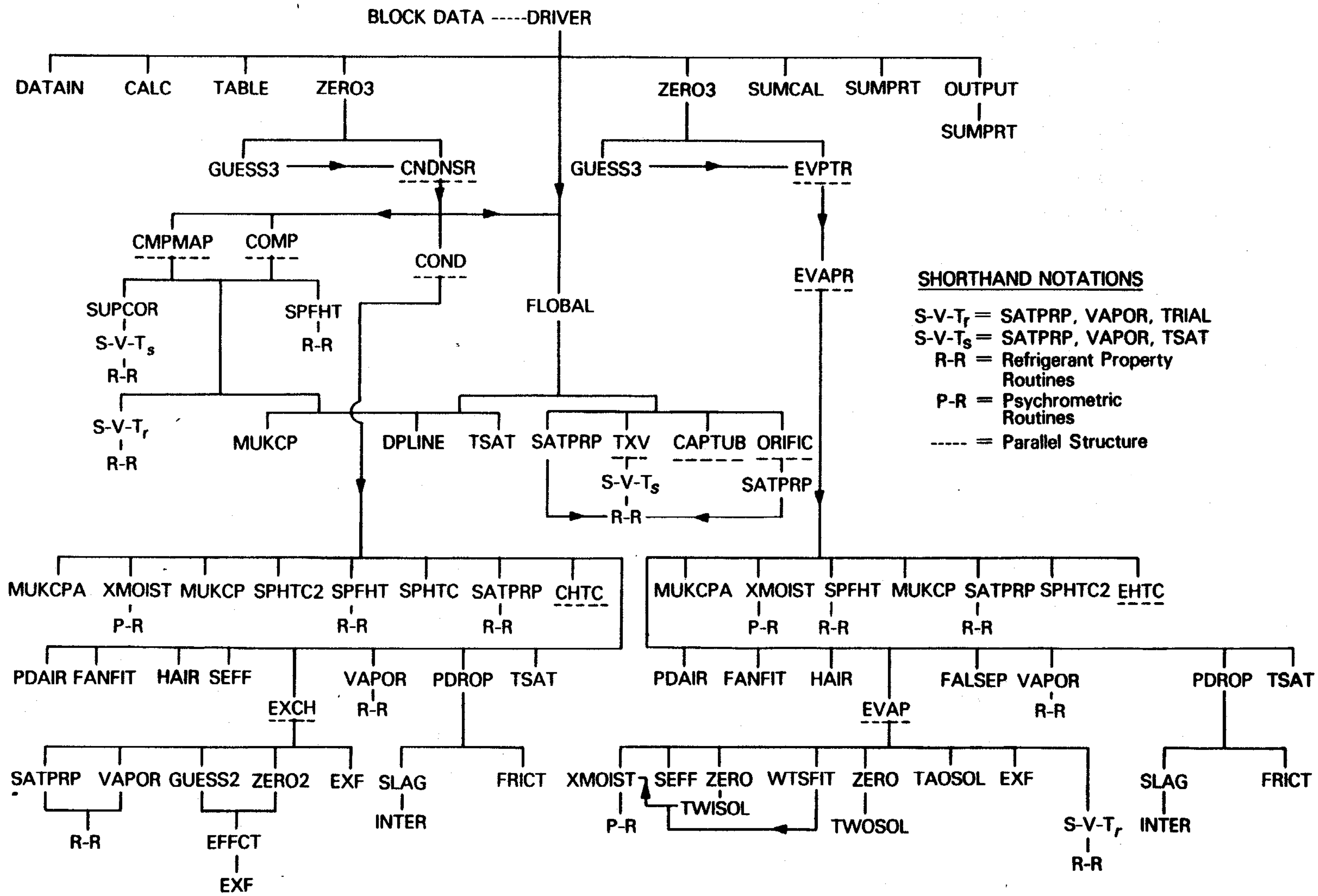

Fig. B.1. Overall structure of the ORNL Heat Pump Design Model -- Mark III version.

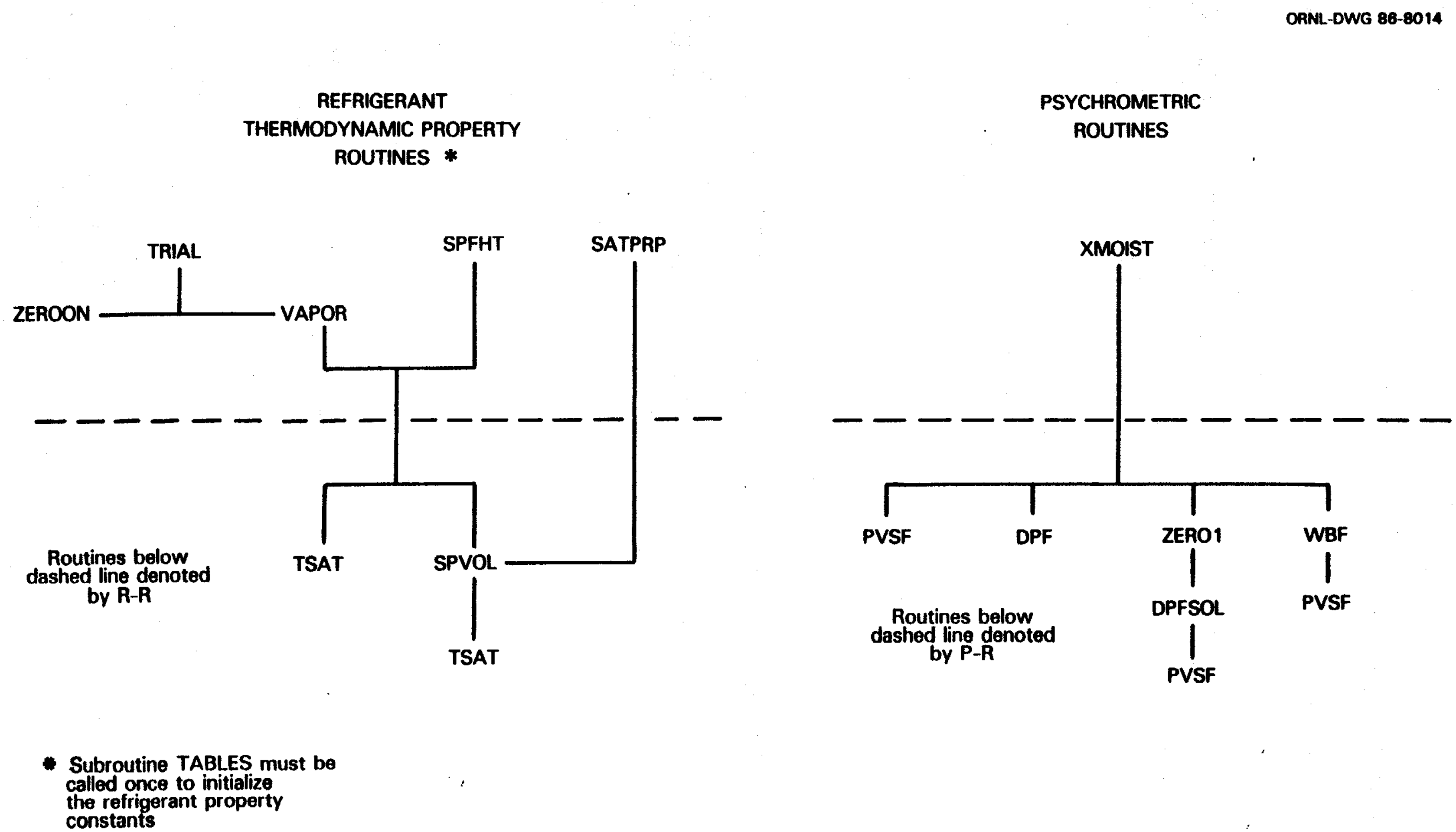

Fig. B.2. Supporting routines.

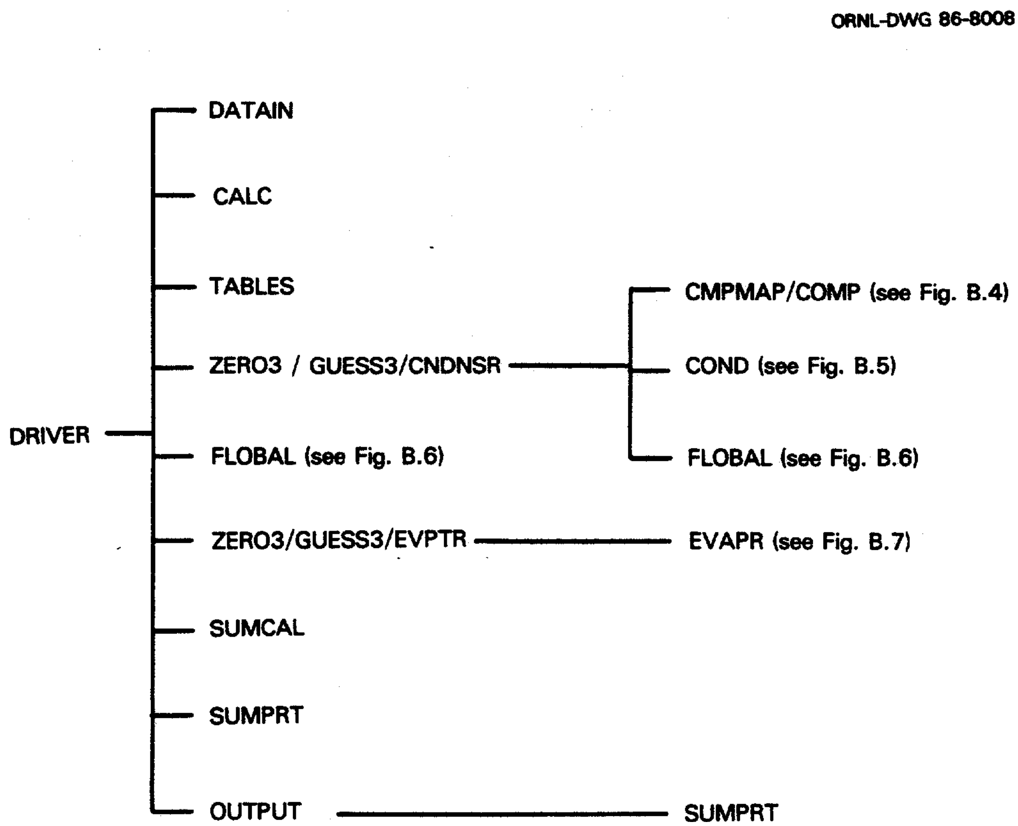

Fig. B.3. Hierarchy of subroutine calls for the ORNL Heat Pump Design Model.

ORNL-DWG 86-8007

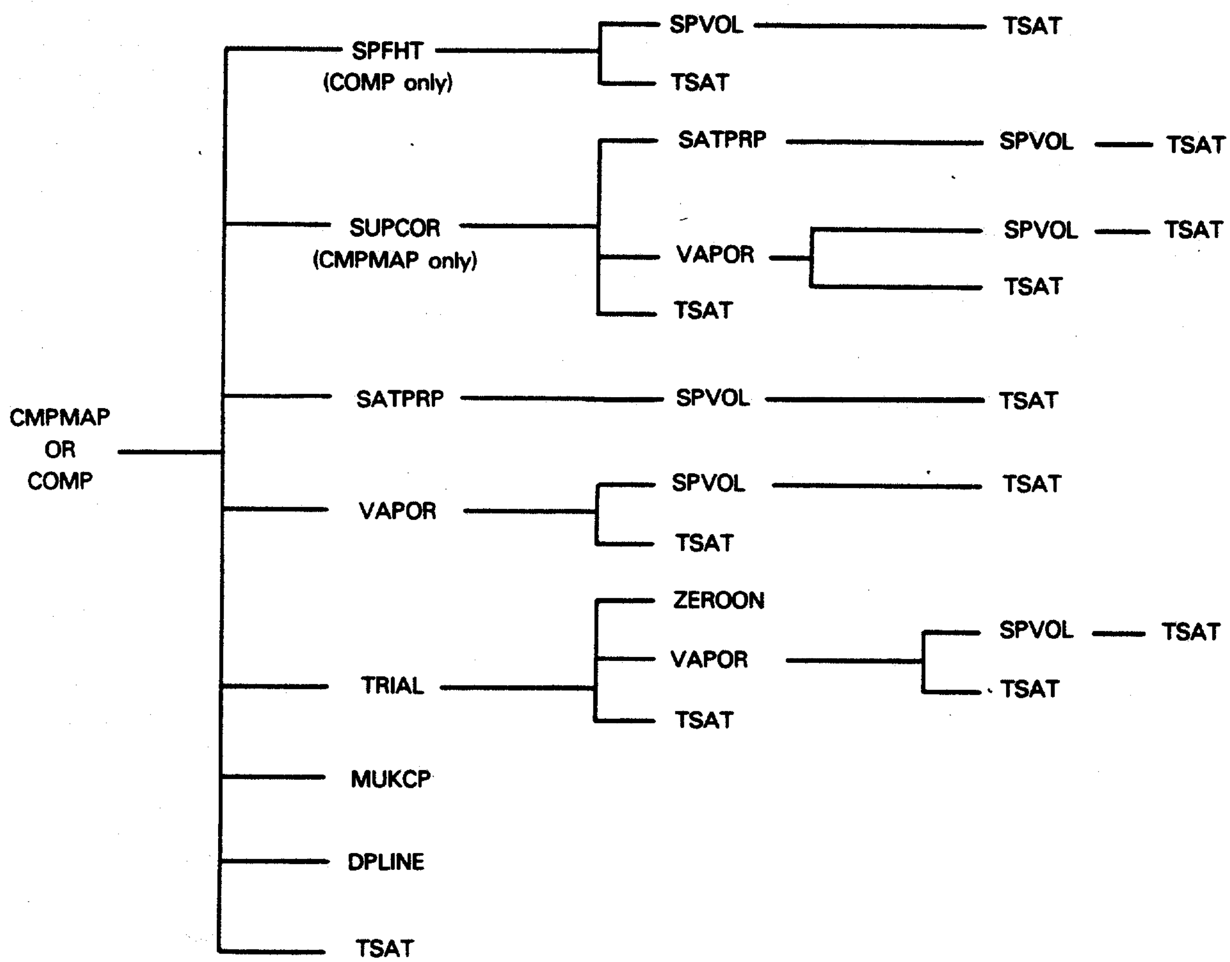

Fig. B.4. Hierarchy of subroutine calls for the compressor models CMPMAP and COMP in the ORNL Heat Pump Design Model.

ORNL-DWG 86-8009

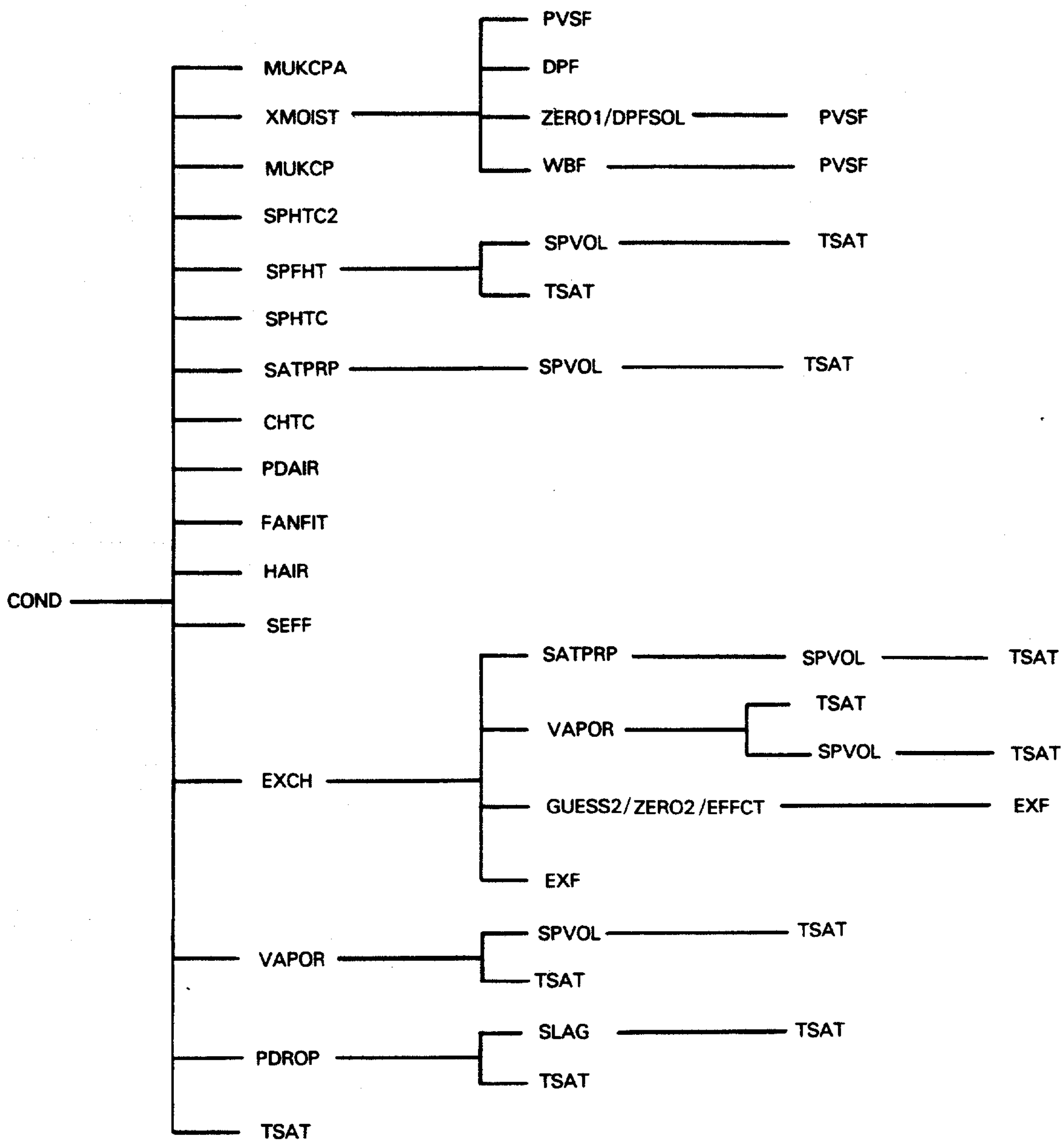

Fig. B.5. Hierarchy of subroutine calls in the condenser model, COND, in the ORNL Heat Pump Design Model.

ORNL-DWG 86-8010

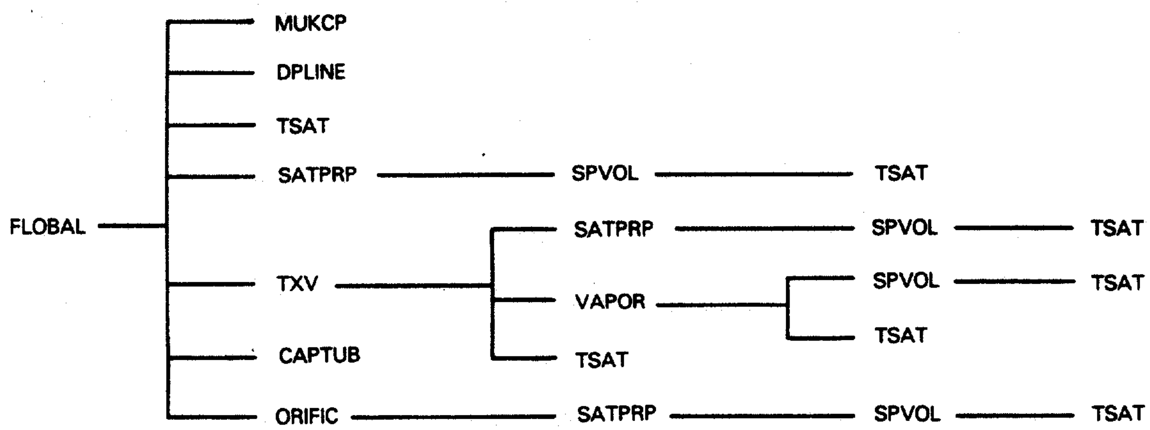

Fig. B.6. Hierarchy of subroutine calls in the flow balancing/flow control routines in the ORNL Heat Pump Design Model.

ORNL-DWG 86-8012

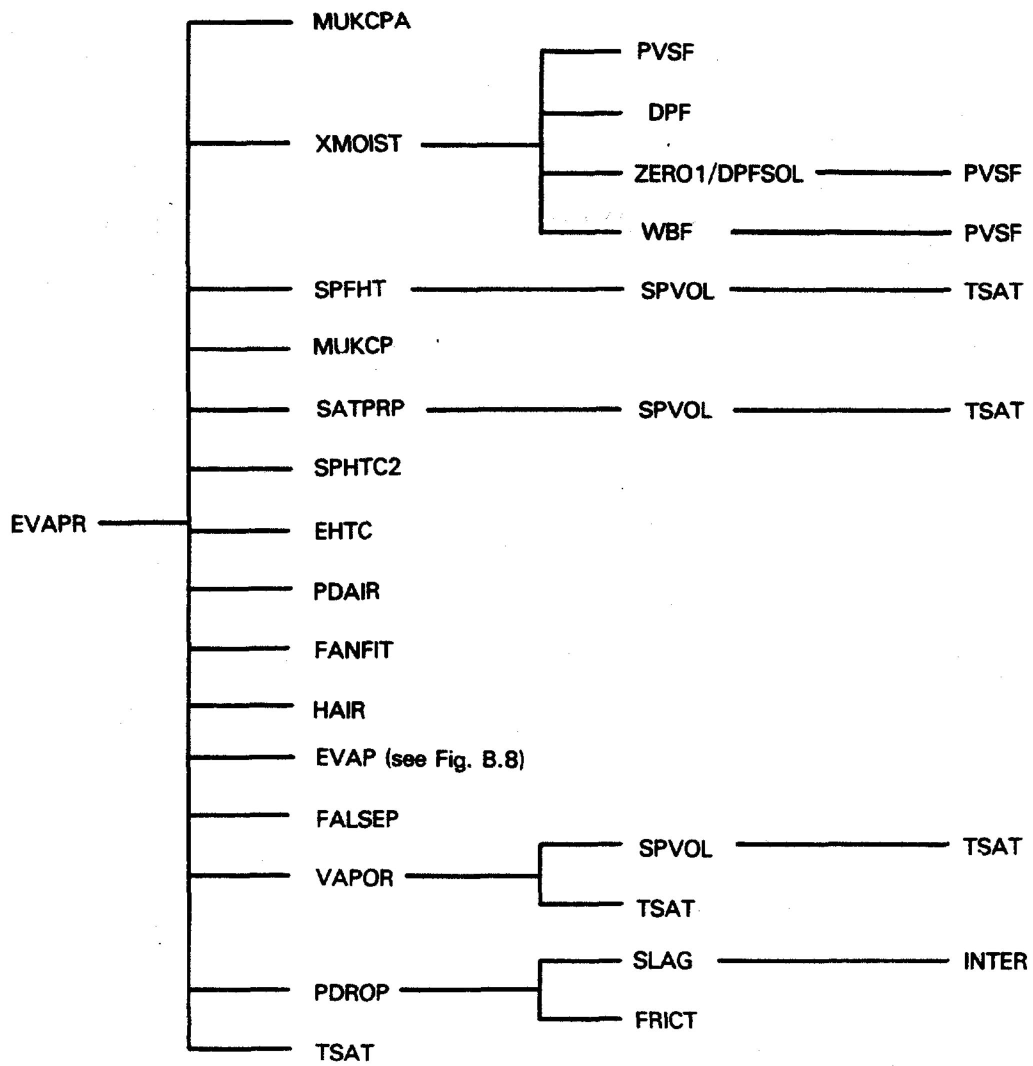

Fig. B.7. Hierarchy of subroutine calls in the evaporator model, EVAPR, in the ORNL Heat Pump Design Model.

ORNL-DWG 86-8011

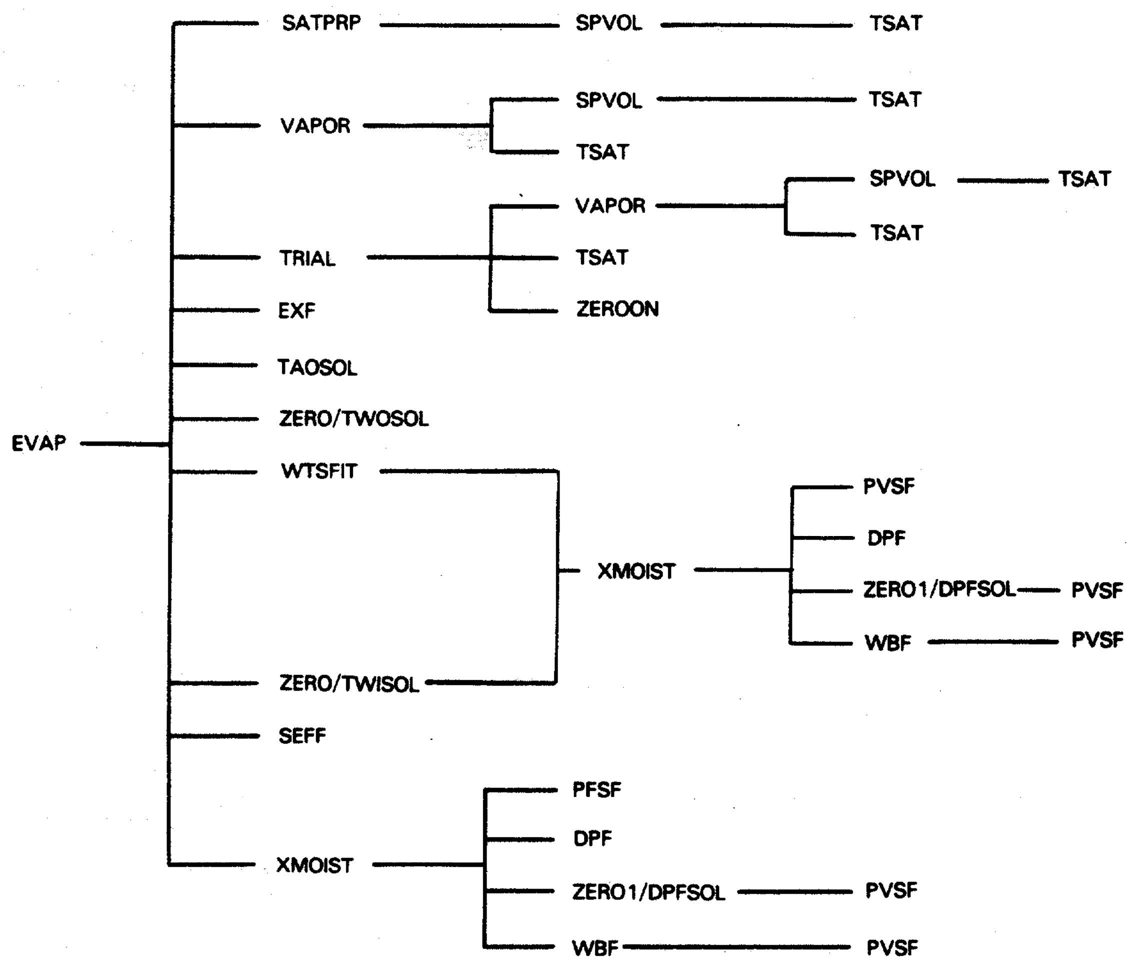

Fig. B.8. Hierarchy of the subroutine calls in the evaporator routine, EVAP, in the ORNL Heat Pump Design Model.